Journal of Non-Crystalline Solids 412 (2015) 11–15

Contents lists available at ScienceDirect

Journal of Non-Crystalline Solids

journal homepage: www.elsevier.com/ locate/ jnoncrysol

Atomic structure of amorphous CdO from first principles simulations

Murat Durandurdu

Department of Materials Science & Nanotechnology Engineering, Abdullah Gül University, Kayseri 38039, Turkey

ARTICLE INFO

Article history:
Received 23 September 2014
Received in revised form 1 January 2015
Accepted 2 January 2015
Available online 8 January 2015

Keywords:
Amorphous;
Ab initio;
Semiconductors;
Molecular dynamics

ABSTRACT

Amorphous CdO (*a*-CdO) is obtained by cooling the liquid at a sufficiently fast cooling rate using first-principles simulations. The topology of the amorphous model is examined using a variety of analyzing techniques. The local structural arrangement of *a*-CdO is found to be partially similar to that of crystalline phase. The model is chemically ordered but consists of a significant amount of coordination defects. *a*-CdO is predicted to be a semiconductor with a band gap energy less than the crystalline state. It is likely that *a*-CdO might serve as a novel electronic material.

1. Introduction

Cadmium oxide (CdO) is a transparent oxide in the visible range and has high-quality structural, electrical and optical properties. It is one of key materials in optoelectronics and has a wide range of technological applications such as solar cells [1], photo transistors [2], diodes [3], transparent electrodes [4] and gas sensors [5]. Because of its important applications it has been studied extensively for last a few decades [6–11].

The ground state of CdO is the octahedrally coordinated cubic rocksalt structure (RS). Therefore it is distinguished structurally from the other IIB–VI semiconductors having tetrahedrally coordinated either wurtzite or zinc blende structures. Interestingly, in spite of the octahedral arrangements of atoms in CdO, it still possesses semiconducting properties with a direct band gap of 2.32–2.5 eV and an indirect band gap of 1.36–1.98 eV, demonstrating that electronic properties of CdO are very much related to those of the other IIB–VI semiconductors [12].

An amorphous form of CdO as a powder also exists in addition to these crystalline modifications. Recently, amorphous nanoclusters [13,14] and amorphous thin films depending on the substrate temperature [15,16] were synthesized experimentally as well. However the atomic structure of *a*-CdO and its electronic properties have not been carefully investigated to date, to our knowledge. Indeed it is quite appealing to see how *a*-CdO forms at the atomistic level and to expose its properties when the technological applications of the crystalline CdO are considered. Here we use an ab initio molecular dynamics approach to generate an *a*-CdO model using the traditional melt-and-quench method and examine the topology of the model using several analyzing techniques. Based upon our results, we propose that *a*-CdO may serve as a new electronic material and find some applications in technology.

2. Methodology

The calculations were carried out using the SIESTA code [17]. The method is based on the density functional theory adopting a localized linear combination of atomic orbital basis sets for the description of valence electrons and norm-conserving nonlocal pseudopotentials for atomic core. The pseudopotentials were constructed using Troullier and Martins scheme [18]. The exchange correlation energy was calculated using the generalized gradient approximation of Perdew, Burke, and Ernzerhof [19]. The double-ξ plus polarized orbitals were employed. A uniform mesh with a plane wave cut-off of 120 Ryd was used to represent the electron density, the local part of the pseudopotentials, and the Hartree and the exchange–correlation potential. This program was found to be very successful in reproducing the high pressure phase of CdO [20]. The molecular dynamics (MD) simulations were performed using the NPT (constant number of atoms, constant pressure, and constant temperature) ensemble. The simulation cell consists of 216 atoms (108 Cd atoms 108 O atoms) with periodic boundary conditions. We used Γ point sampling for the Brillouin zone integration. The initial rocksalt structure was melted at 2500 K (5.0 ps) and then the liquid state was gradually cooled to 2000 K in a period of 5.0 ps. At this temperature, the structure was thermalized for 10.0 ps. To ensure that the 10 ps is enough to capture the dynamics of the liquid state, we studied the mean square displacement (MSD) for last 1000 configurations using the isaacs program [21] and presented it in Fig. 1. The MSD was proportional to t^2 up to 40 fs suggesting ballistic motion. Beyond this time, it exhibited a linear behavior, indicating that the liquid was in a diffuse state. The linear behavior of the MSD also specified that liquid reached a state of equilibrium. Fitting the diffusive part with a straight line and using the Einstein relation, $<(r(t) - r(0))^2> = 6tD$, we obtained a value of 6.6×10^{-5} cm^2/s for

E-mail address: murat.durandurdu@agu.edu.tr.

http://dx.doi.org/10.1016/j.jnoncrysol.2015.01.001
0022-3093/

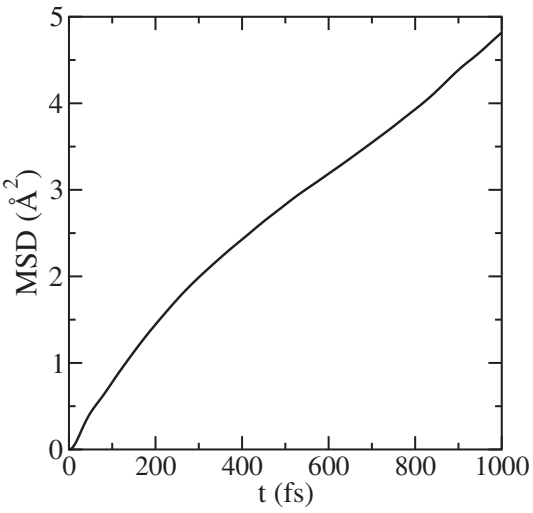

Fig. 1. Mean square displacement at 2000 K.

the diffusion constant *D*. The liquid state was gradually cooled to 300 K using different cooling rates. The amorphous state was only achieved at a sufficiently fast cooling rate of 0.5 K/fs. With other cooling rates, the crystallization into a RS phase as shown in Fig. 2 was observed around 400–600 K depending on the cooling rates in our simulations. The amorphous network at 300 K was finally relaxed. Each time step is one femtosecond (fs). Temperature was controlled using the velocity rescaling method. The volume of the supercell was equilibrated using the Parrinello and Rahman technique [22] without allowing any shear deformation.

3. Results and discussion

The solidification mechanism can be characterized using various analyzing techniques. The first quantity we would like to focus on here is partial pair distribution functions (PPDFs), a commonly used practical technique to determine the interatomic correlations particularly for disordered systems. Fig. 3 shows PPDFs as a function of temperature. In all pairs at different temperatures, a well defined nearest neighbor peak and a rapid loss of the interatomic correlations are observed, as expected, due to the lack of long-range order. From the figure, the sharpening of the first Cd–O peak is clearly evident with decreasing temperature, suggesting more order around Cd and O atoms. The similar tendency is also determined in the first peak of both Cd–Cd and O–O but it is not as severe as in the Cd–O correlation. Interestingly, the position of the first peaks is found to be not too sensitive to temperature, that is, it does not noticeably alter with temperature. Here it can be concluded that the microstructures of liquid and amorphous CdO are *roughly* similar to each other.

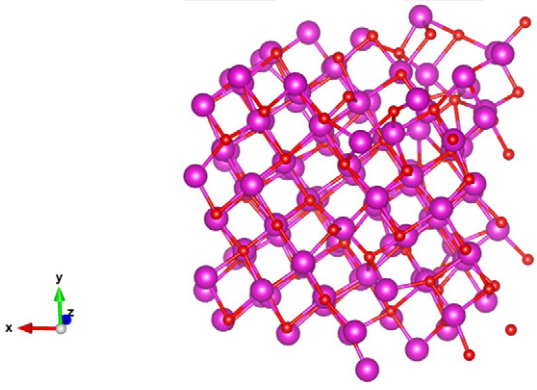

Fig. 2. Crystalline structure formed during quenching from the melt. Big and small spheres are Cd and O atoms, respectively.

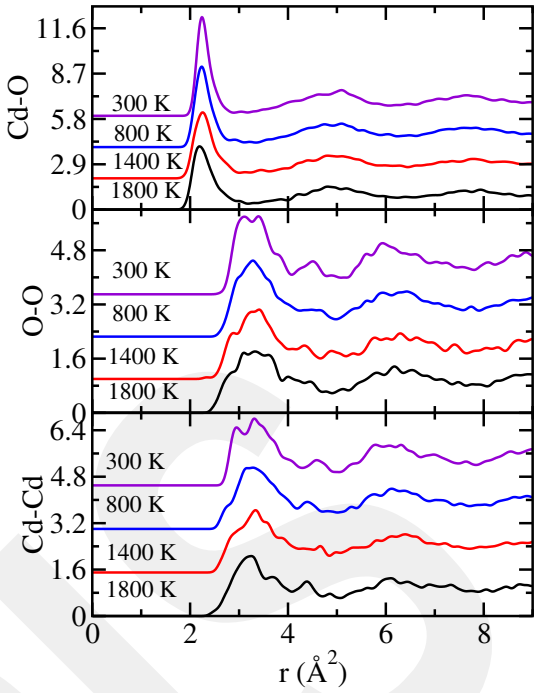

Fig. 3. Temperature dependence of partial pair distribution functions (PPDFs) during the solidification.

To compare the local atomic arrangements of *a*-CdO (relaxed) with those of the crystalline RS structure, we also study PPDFs of the RS phase and present them in Fig. 4. The disordered nature of amorphous state results into broad and weak peaks relative to the crystal. As can be seen from the figure, the first sharp peaks of both *a*-CdO and the crystal are roughly located at the same positions. The first Cd–O neighbor separation is located around 2.26 Å, which is slightly shorter than the Cd–O distance of 2.34 Å formed in the crystal. On the other hand, the Cd–Cd and O–O pairs split into two peaks (will be called subpeaks). For Cd–Cd (O–O) correlation, the first subpeak's position is at 2.93 Å (3.06 Å) and the second one is around 3.32 Å (3.4 Å). The splitting of the peak in the Cd–Cd and O–O correlations means that there are two different characteristic length scales between nearest Cd

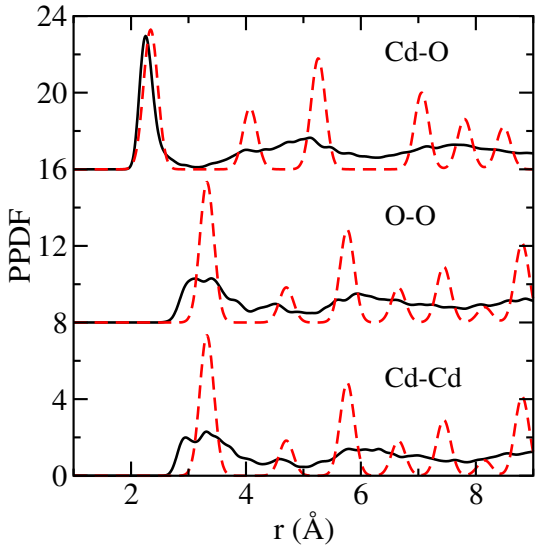

Fig. 4. Partial pair distribution functions (PPDFs) of *a*-CdO (solid line) and RS structure (dashed line).

(O) neighbors in the amorphous and *a*-CdO apparently has a local environment partially different from the crystalline morphology.

In order to understand the origin of the splitting, the imaginary Cd–Cd and O–O bonds for 3.1 Å and 3.2 Å distances (subminimums) respectively are created in the model and each topological unit that forms the imaginary bonds for these certain separations is carefully analyzed. As shown in Fig. 5, the splitting is due to the angle distortions. For the case of bond bending (bending of plane), both Cd–Cd and O–O separations decrease, relative to the crystal, and produce the first subpeaks. For the case of the bond distortions with almost no bond bending, the square lattice becomes a diamond like lattice and the distance between atoms located at larger angles decreases while the distance between atoms positioned at small angles increases. These types of angular distortions result in two Cd–Cd or O–O separations and hence the splitting of these correlations.

To further analyze the topology of the model, we calculate the Cd–O–Cd and O–Cd–O bond angle distribution functions using the cutoff radii of 3.08 Å (amorphous) and 3.18 Å (liquid) for the Cd–O pair correlation and plot them in Fig. 6. The model has very broad bond angle distribution functions ranging from 60° to 180° for *a*-CdO and from 45° to 175° for the liquid CdO in stark contrast to two sharp peaks at 90° (strong) and 180° (weak, relative to 90°) in the crystal. As temperature is decreased, the peak near 90° is sharpened. The angles around 90° and 180° can be interpreted as the tendency of the amorphous model to preserve its crystalline like short-range order and to form an octahedral structure. One can also notice that Cd atoms have a more trend to form a local structure similar to the crystal since the peak's intensity around 90° in the O–Cd–O is larger than that of Cd–O–Cd.

Coordination numbers (CNs), total and partials, are another important structural parameter for materials. Here we analyze the average CNs using the Voronoi polyhedral technique [23], more sensitive approach than the PPDF method to determine CNs in disordered materials. This approach also provides valuable information about local structural units and their connectivity in amorphous structures. A Voronoi polyhedron can be constructed by connecting perpendicular bisectors between a central atom and all of its neighboring atoms and is represented by indices $<n_3, n_4, n_5, n_6,\ldots>$ where n_i offers the number of i-edge faces of polyhedron and Σn_i gives the total CN. Fig. 7 presents the types and fractions of Cd and O-centered polyhedrons for the liquid state at 2000 K and amorphous state (relaxed). As seen from the figure, sixfold coordinated clusters with an index of <0, 6, 0, 0>, and fivefold coordinated

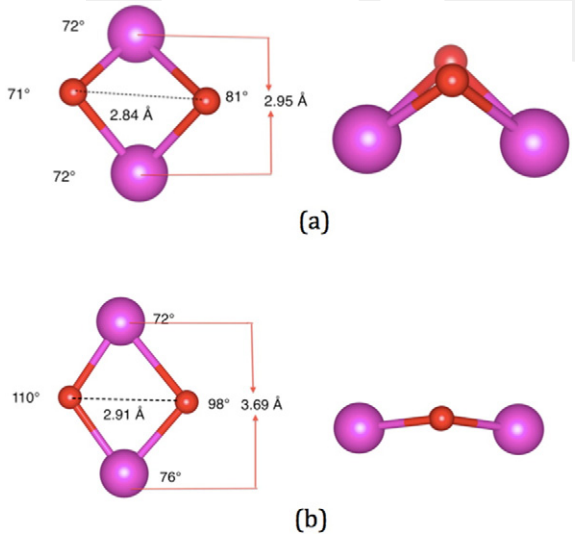

Fig. 5. Atomistic origin of splitting in the Cd–Cd and O–O correlations. Topological units with angle distortions (a) bond bending (b) without bond bending. The clusters are viewed in two different directions to distinguish to their differences. Big and small spheres are Cd and O atoms, respectively.

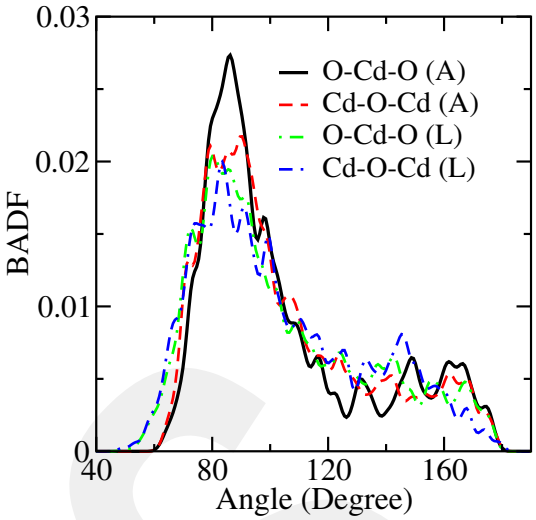

Fig. 6. Cd–O–Cd and O–Cd–O bond angle distribution functions of liquid (L) and amorphous (A) CdO.

polyhedrons having an index of <2, 3, 0, 0> and <4, 0, 0, 0> are the major building units around both Cd and O atoms in the short-range order of liquid CdO. With decreasing temperature, the fraction of <4, 0, 0, 0> polyhedra decreases considerably and the <0, 6, 0, 0> and <2, 3, 0, 0> clusters become dominated for *a*-CdO. Additionally, O atoms form <2, 2, 2, 0> structures with a small frequency. The <0, 6, 0, 0> structure is an octahedron (see Fig. 8). The five fold coordinated <2, 3, 0, 0> cluster might be considered as an incomplete octahedron with missing one atom. It has a central atom surrounded by five atoms. This cluster is pyramid shaped (see Fig. 8). The central atom and its four neighboring atoms are on the same plane (the base of the pyramid), similar to a cross-sectional view of the face centered cubic structure, and its one neighboring atom is on the plane passing through the top vertex and perpendicular to the base of the pyramid. Although the <2, 2, 2, 0> polyhedron has a central atom having six neighbors, it is closely related to the <2, 3, 0, 0> cluster. The central atom and its four neighboring atoms are on the same plane, similar to the <2, 3, 0, 0> polyhedron and its two neighboring atoms are on a different plane. These two planes are perpendicular to each other. If one of the two neighboring atoms is removed, the <2, 2, 2, 0> cluster becomes a very

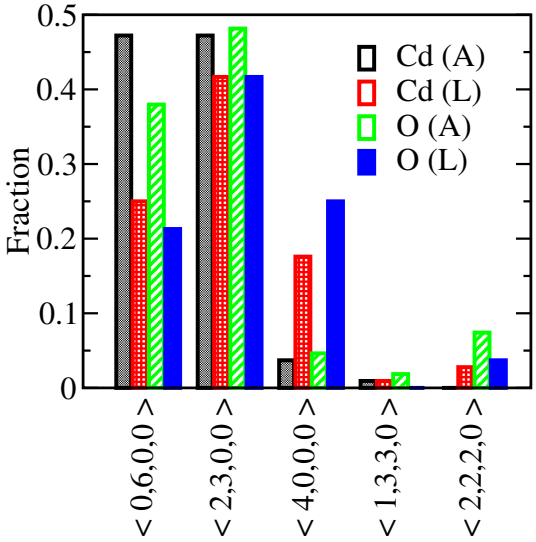

Fig. 7. Distribution of Voronoi clusters for Cd and O atoms.

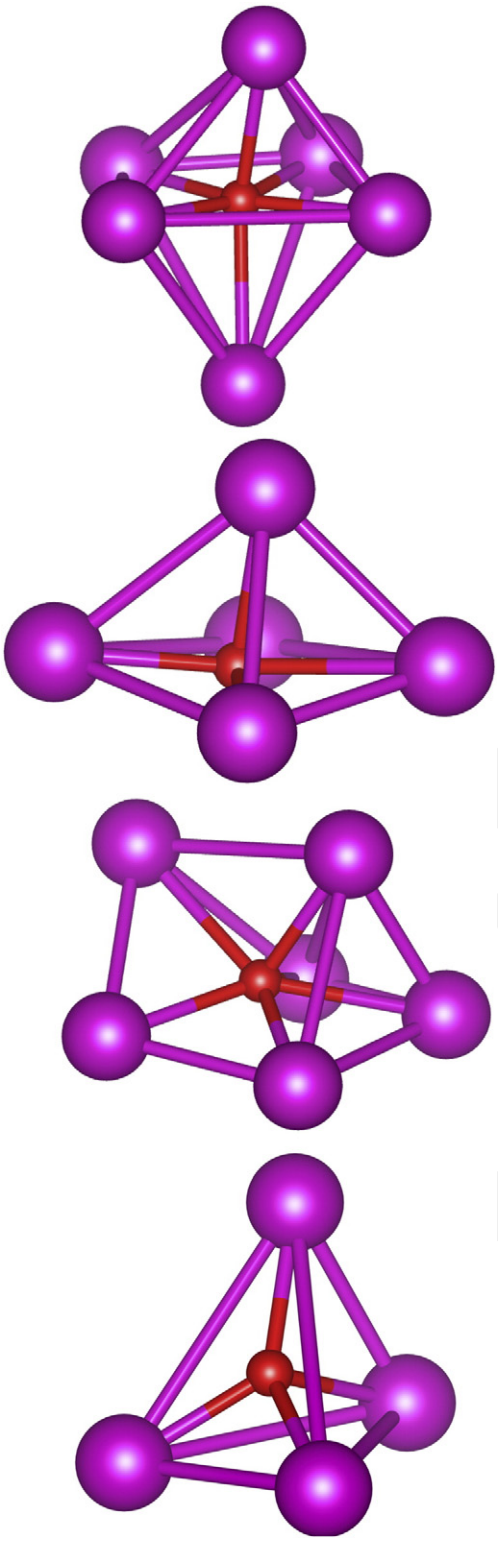

Fig. 8. Typical O-centered <0, 6, 0, 0>, <2, 3, 0, 0>, <2, 2, 2, 0> and <4, 0, 0, 0> clusters formed in CdO system. Big and small spheres are Cd and O atoms, respectively. Noted imaginary bonds between Cd–Cd are formed to have a clear description of these clusters.

deformed <2, 3, 0, 0> polyhedron. Missing one atom at the base of the pyramid (<2, 3, 0, 0>) yields to the <4, 0, 0, 0> cluster. We should note here that the definition of these clusters is for ideal cases. In liquid and amorphous states, they are distorted and hence they do not have uniform bond distances and angles. Noted that the RS phase has only one type polyhedron with the index of <0, 6, 0, 0> and hence the liquid

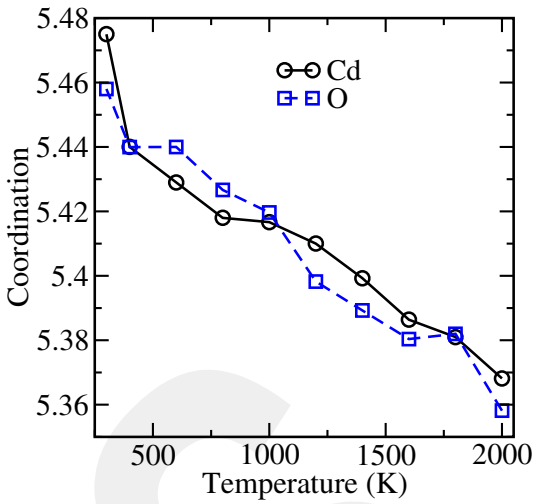

Fig. 9. Average CNs as a function of temperature.

and amorphous states carry structurally some characteristic of the RS crystal. The temperature dependence of the average CNs is illustrated in Fig. 9. The CN of Cd and O atoms computed to be 5.36 and 5.35, respectively for liquid CdO. The CNs correlate with temperature and four-to-five and five-to-six coordination modifications occur stepwise in the system during the solidification process, yielding a gradual increase in the CNs and an average CN of 5.46 for Cd atom and 5.47 for O atom at 300 K.

The fivefold coordination, similar to the pyramid shaped in *a*-CdO, frequently occurs in silicate glasses [24] and TiO_2 (Ref. [25]) and the average CN is found to be lower in amorphous states than in their corresponding crystalline structures in these systems. Additionally the liquid state of these materials has a lower average CN, relative to the crystalline counterparts. The adopting lower coordination is perhaps a common characteristic of disordered forms of octahedrally coordinated oxide materials. Consequently the observation of the coordination defects (undercoordinated atoms), a lower average CN and partially different structure is completely typical for CdO.

The Voronoi analysis additionally suggests that *both* states of CdO are chemically ordered, that is, no Cd–Cd and O–O homopolar bonds exist in the model, which can be attributed to the ionicity of CdO.

We finally study the electronic structure of the amorphous model, which can be described by electron density of state (EDOS). The calculated EDOS of *a*-CdO and the RS phase is presented in Fig. 10.

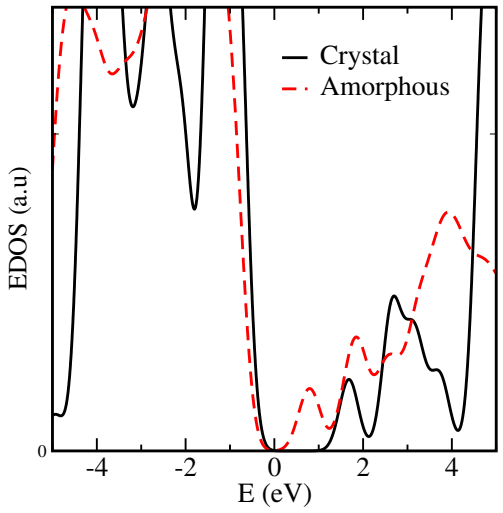

Fig. 10. Electron density of state (EDOS) near the band gap. Fermi level is shifted to zero.

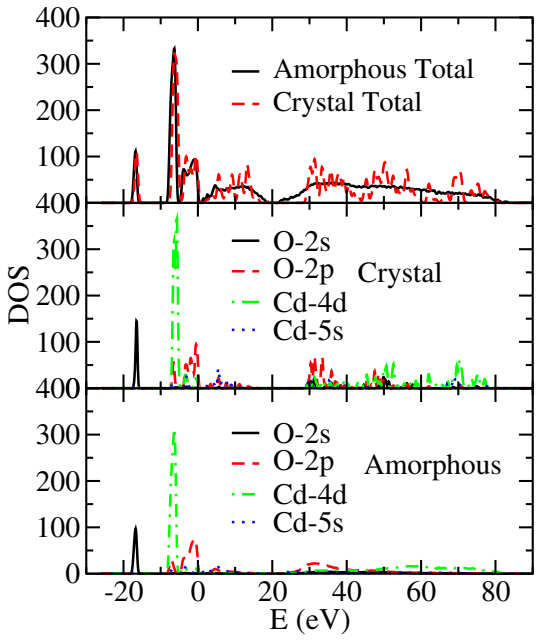

Fig. 11. Total density of state (DOS) and partial density of states (PDOS). Fermi level is shifted to zero.

Surprisingly *a*-CdO still presents semiconducting properties even though it has a significant amount of coordination defects. The theoretical band gap energy of *a*-CdO is predicted to be about 0.45 eV, which is less than 1.35 eV calculated for the RS phase. The experimental gap energy would be larger than this value since DFT underestimates band gap energy. For a deeper understanding, we also analyze the partial density of states (PDOS) given in Fig. 11. The energy band levels around −20 eV are due to O-2s states. The upper valance band near the Fermi Level consists of O-2p states. The band with the strongest intensity is dominated by Cd 4d states. The lower conduction band near the Fermi level has contributions from both O-2p and Cd-5s states. These findings are similar to what has been observed for the crystalline phase in a previous study [11].

Note that the band gap of *a*-CdO might be easily altered by either simply improving the coordination defects or inducing nanostructures in the amorphous matrix. Both can be achievable possibly using thermal treatments. If its band gap can be engineered experimentally to desired values, then *a*-CdO might find some important electronic and optoelectronic device applications.

4. Conclusions

a-CdO is modeled from the melt using an ab initio technique. The model is found to be chemically ordered but highly defective. Its average coordination is lower and it is partially different than the RS state. Despite a substantial amount of coordination defects, *a*-CdO still presents semiconducting properties. Based on our findings, it is probable that *a*-CdO might find some uses in electronic and optoelectronic devices. Yet additional works, in particular, experimental works are definitely needed to fully reveal the properties of *a*-CdO.

Acknowledgment

This work was supported by TÜBİTAK (the Scientific and Technical Research Council of Turkey) under BİDEB-2232 program.

References

[1] S. Kose, F. Atay, V. Bilgin, I. Akyuz, Int. J. Green Energy 1 (2004) 353.
[2] R. Kondo, H. Okimura, Y. Sakai, Jpn. J. Appl. Phys. 10 (1971) 1547.
[3] F.A. Benko, F.P. Koffyberg, Solid State Commun. 57 (1986) 901.
[4] A. Shiori, Jpn. Pat., No. 7 (1997) 909.
[5] D.R. Lide (Ed.), CRC Handbook of Chemistry and Physics, 77th editionCRC Press, Boca Raton, 1996–1997, pp. 12–97 (3/278).
[6] R.J. Guerrero-Moreno, N. Takeuchi, Phys. Rev. B 66 (2002) 205205.
[7] J.J. Mudd, Tien-Lin Lee, V. Muñoz-Sanjosé, J. Zúñiga-Pérez, D. Hesp, J.M. Kahk, D.J. Payne, R.G. Egdell, C.F. McConville, Phys. Rev. B 89 (2014) 035203.
[8] C. Rödland, A. Schleife, Phys. Status Solidi (a) 211 (2014) 74.
[9] A. Aïdouni, A. Zaouiland, M. Ferhat, Phys. Status Solidi B 251 (2014) 1426.
[10] A. Jemmy Cinthia, G. Sudhapriyang, R. Rajeswarapalanichamy, M. Santhosh, Procedia Mater. Sci. 5 (2014) 1034.
[11] G. Yao, X. An, H. Lei, Y. Fu, W. Wu, Model. Numer. Simul. Mater. Sci. 3 (2013) 16.
[12] J.C. Boettger, A.B. Kunz, Phys. Rev. B 27 (1983) 1359.
[13] B.S. Zou, V.V. Volkov, Z.L. Wang, Chem. Mater. 11 (1999) 3037.
[14] V.V. Volkov, Z.L. Wang, B.S. Zou, Chin. Phys. 9 (2000) 667.
[15] B.A. Ezekoye, V.A. Ezekoye, P.O. Offor, S.C. Utazi, Int. J. Phys. Sci. 8 (2013) 1597.
[16] R.S. Rusu, G.I. Rusu, J. Optoelectron. Adv. Mater. 7 (2005) 1511.
[17] P. Ordejón, E. Artacho, J.M. Soler, Phys. Rev. B 53 (1996) 10441.
[18] N. Troullier, J.L. Martins, Phys. Rev. B 43 (1997) 1993.
[19] J.P. Perdew, K. Burke, M. Ernzerhof, Phys. Rev. Lett. 77 (1996) 3865.
[20] M. Durandurdu, Europhys. Lett. 84 (2008) 66003.
[21] S. Le Roux, V. Petkov, J. Appl. Crystallogr. 43 (2010) 181.
[22] M. Parrinello, A. Rahman, Phys. Rev. Lett. 45 (1980) 1196.
[23] L. Yang, G.Q. Guo, L.Y. Chen, S.H. Wei, J.Z. Jiang, X.D. Wang, Phys. Rev. B 63 (2010) 879–882.
[24] G.S. Henderson, G. Calas, J.F. Stebbins, Elements 2 (2006) 269.
[25] B. Prasai, B. Cai, D.A. Drabold, M.K. Underwood, J.P. Lewis, J. Mater. Sci. 47 (2012) 7515.